BIODISTRIBUTION OF DOXORUBICIN-LOADED SUCCINOYL CHITOSAN NANOPARTICLES IN MICE INJECTED VIA INTRAVENOUS OR INTRANASAL ROUTES

Anastasia A. Zubareva, Tatyana S. Shcherbinina, Valery P. Varlamov, Elena V. Svirshchevskaya*

Centre «Bioengineering» RAS,
Prospect 60-Letia Oktyabrya 7/1, Moscow, Russia
e-mail: enzyme@biengi.ac.ru

**Shemyakin and Ovchinnikov Institute of Bioorganic Chemistry RAS,*
Ul. Miklukho-Maklaya, 16/10, Moscow, Russia

Abstract
Chitosan (Chi) is an extremely promising natural biopolymer with remarkable potency for the development of drug and vaccine delivery nanosystems. Various Chi derivatives are used to form nanoparticles (NPs) with unique properties. However, the efficacy of the therapy delivered by Chi NPs depends significantly on NP biodistribution in the body. The aim of this study was the analysis of biodistribution of NPs formed by succinoyl Chi and loaded with doxorubicin (SCNP-DOX). We compared the distribution of free DOX and SCNP-DOX after intravenous (i.v.) and intranasal (i.n.) delivery into tumour-bearing mice. Distribution of DOX and SCNP-DOX was comparable after i.v. injection while they differed significantly after i.n. instillation.

Key words: *succinoyl chitosan nanoparticles, doxorubicin, biodistribution.*

DOI: 10.15259/PCACD.19.18

1. Introduction

Currently, chitosan and chitosan derivative nanoparticles (NPs) are intensively studied as drug delivery systems due to the high safety, biodegradability, biocompatibility and availability of multiple reactive groups needed for derivation in chitosan [1]. Various molecules such as proteins [2, 3], peptides [4], chemotherapeutic substances [5], vitamins [6] and others can be incorporated into ChiNPs. In spite of the careful characterisation of nanosystems *in vivo* and *in vitro,* there is little information on the biodistribution of NPs in the body, which can partly be explained by the complexity of the system analysis.

Most ChiNPs biodistribution studies are conducted in tumour growth models and use an intravenous (i.v.) delivery route for NPs injections [7 - 10]. To track the NPs distribution in tissues, fluorescent dyes such as fluorescein isothiocyanate (FITC) or rhodamine (Rho), conjugated or loaded by passive sorption, are often used [7, 8]. Son et al. demonstrated an increased accumulation of glycol-chitosan nanoagreggates conjugated with FITC in kidney, tumour, and liver, with marginal quantities in other organs [7]. However, FITC excitation wavelength is very close to the auto-fluorescence spectrum. The authors estimated FITC quantity without the subtraction of auto-fluorescence of organs, which is different in each tissue. In the same work, the authors also prepared glycol-chitosan nanoaggregates with doxorubicin (DOX) which possesses self-fluorescence in red region with better resolution between DOX and auto-fluorescence. Another study conducted by Chunbai He et al. demonstrated the difference between the biodistribution of positively and negatively charged ChiNPs [8]. In this work, Rho label was used to track the NPs. The authors found that positively charged ChiNPs accumulated in the liver and spleen while carboxymethyl ChiNPs, negatively charged, accumulated predominantly in tumours. Again, no auto-fluorescence control was subtracted. In both studies, NP extraction from tissues was conducted using saline, while solvents such as chloroform/methanol and others could extract higher amounts of NPs from tissues [9].

High performance liquid chromatography (HPLC) is an alternative method used to study the biodistribution of different NPs. HPLC lacks the problems with auto-fluorescence, as it determines the concentrations of a specific compound such as DOX or FITC. Biodistribution of N-octyl-O-sulphate chitosan NPs loaded with paclitaxel (PTX), the concentration of which in organs was analysed by HPLC, demonstrated PTX distribution in different organs in a comparable manner with major accumulation in the liver [10]. However, HPLC is inconvenient for the study of multiple samples.

Intranasal (i.n.) delivery is a perspective route of NPs injection, especially for the treatment of brain tumours due to the safety and non-invasive nature of injections and also due to a ready contact with blood vessels in nasal mucosa closely located to brain barriers. Intranasal delivery prevents NPs from enzyme degradation in the liver, leading to a better bioavailability. ChiNPs can be used for the treatment of inflammation of the nasal cavity, as well as brain tumours or neurodegenerative disorders. There are several publications demonstrating the increased delivery of drugs by NPs into the brain through the blood-brain barrier (BBB) [11]. The only work on the biodistribution of ChiNPs delivered by the i.n. route was conducted using radioactive technetium (99mTc). The authors demonstrated

a completely different from i.v. route for NPs distribution with the major quantity in the intestine and stomach and equal amounts in organs such as the liver, kidney and lungs, among others. A slight yet significant increase of NPs transport into brains was found. We believe that other studies are required to verify the biodistribution of ChiNPs after i.n. route of delivery [12].

The aim of this work was to study the biodistribution of succinoyl chitosan NPs loaded with doxorubicin (SCNP-DOX) and injected either i.v. or i.n. into mice with tumours. DOX is an anti-tumour antibiotic possessing a fluorescent group which was used to register the biodistribution.

2. Materials and methods

2.1. Materials

Succinoyl chitosan (SC) (substitution degree 70-80%) (***Figure 1***) was prepared from chitosan with M_W 340 kDa (ZAO «Bioprogress», Moscow region, Russian Federation). SC was purified by precipitation with 30% CH_3COOH (Reachim, Moscow, Russian Federation) before use. Doxorubicin hydrochloride (TEVA, Netherlands) and calcium chloride (Sigma, USA) were used in the study.

2.2. Methods

2.2.1. Preparation of succinoyl chitosan nanoparticles (SCNPs) by coacervation method

SCNPs were formed by the coacervation method, as previously published by our group [13, 14]. Briefly, 1% $CaCl_2$ (Sigma) was added dropwise to 0.15% SC pre-diluted in bi-distilled water under constant stirring for 20 min at 30 rpm and 22°C. SCNGs were separated by centrifugation (14,000rpm, 20 min) and then re-suspended in bi-distilled water. Aliquots of the suspension were freeze-dried to estimate the amount of SC inserted in the nanostructures. The yield of particles was about 8%.

2.2.2. Sorption of DOX on SCNPs

To prepare SCNPs loaded with DOX, 4 mg of DOX in 0.03 ml DMSO was gradually added to 0.5 ml of SCNP dispersion in deionized water (400 μg/ml). The solution was supplemented with deionized water to a total volume of 1 ml. The final concentration of nanoparticles in the solution was 200 μg/ml. The process of sorption was carried out under stirring (30 r.p.m.) at 22 °C for 1 h. The particles loaded with DOX were separated by

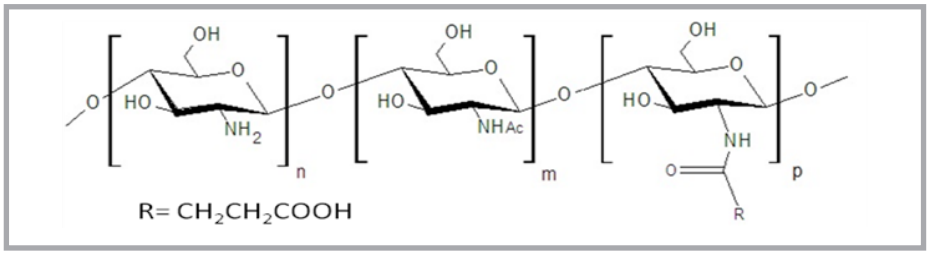

Figure 1. *Chemical structure of succinoyl chitosan.*

centrifugation at 14,000×g for 20 min and then resuspended in 1 ml of 0.9% NaCl solution, incubated at 22 °C for 30 min, and finally were separated by centrifugation again. The quantity of the adsorbed DOX was determined by spectrophotometry at a wavelength of 481 nm. The effective sorption (ES) of doxorubicin was 25%, which was determined using the following equation:

$$ES = \frac{m_0 - m_1}{m_0} \cdot 100\%,$$

where m_0 - total doxorubicin quantity and m_1 - free doxorubicin quantity.

2.2.3. Characterisation of prepared NPs

2.2.3.1. Dynamic Light Scattering (DLS)

The mean size and zeta potential of NPs were determined by 90 Plus Particle Size Analyser (Brookhaven Instruments Corporation, Vernon Hills, IL, USA). Parameters of nanoparticles were measured in bi-distilled water at a scattering angle 90° and 661 nm wavelength. The zeta potential of the system was determined in 10 mMKCl (Sigma) using identical equipment with an additional ZetaPALS apparatus. Measurements were performed at 25.0 ± 0.1 °C.

2.2.3.2. Laser Interference Microscopy

ChiNPs visualisation was accomplished with a MIM-321 laser interference microscope (AMPHORA Laboratories LLC, Moscow, Russian Federation). The spatial resolution up to 0.1 nm vertical (Z) and 10 nm lateral (XY) was achieved with Olympus MPLFLN 100 × 0.9 dry objective. The 10 µl diluted solution of NGs was placed on the mirror glass and dried. The gradient filtering was applied to visualise the shape and the internal structure of ChiNP.

2.2.3.3. Nanoparticle Tracking Analysis (NTA)

NTA experiments were performed using a NanoSight NS500 system (NanoSight, Wiltshire, UK). Video images of particle movement under Brownian motion were analysed by NTA analytical software version 2.2. The measurements were made at room temperature and 60 s capture of video clips.

2.2.4. Biodistribution study

For biodistribution experiments, C57BL/6 mice (Central Farm, Moscow region), 18 - 20 g in weight, were inoculated in a fat pad #4 with 10E6 of Wnt-1 tumour cells obtained from a donor mouse [15]. All experiments were approved by the Institution animal commission.

When tumour mass reached 1 g, mice were randomly divided into 5 groups (n = 3/group): control mice received 200 µl of saline; experimental mice received either 25 µg/mouse of free DOX in 200 µl or SCNP-DOX (25 µg of DOX per 200 µl of SCNPs) injected i.v. into eye orbital sinus or via 10 i.n. instillations of 20 µl every 30 min, each time alternating nostrils. Mice were euthanised by cervical dislocation 1 hour after the last i.n. injection or after the only i.v. injection. Heart, liver, kidney, lungs and spleen were collected into saline. To analyse the quantity of DOX, organs were homogenised using metal meshes and 700 µl aliquots were mixed with 1300 µl of the extraction buffer (0.3 N HCl, 70% C_2H_5OH). Plates with homogenates were incubated at 4 °C overnight; samples were transferred into

eppendorf tubes and centrifuged at 10,000 r.p.m. for 20 min. The transparent phase was collected for the analysis using a fluorescent plate reader (Promega Glomax Multi, USA) [15]. Free DOX dissolved in the same extraction buffer was used to calibrate the amount of DOX extracted from the tissues using a 525 nm cut-off filter. The amount of DOX extracted from the tissues was calculated using a linear approximation of the DOC titration curve after subtraction of auto-fluorescence measured in samples of organs prepared from control mice.

2.2.5. Statistics

Statistical analysis was performed using Student's t-test. Comparison values of $p < 0.05$ were considered statistically significant.

3. Results and discussion

3.1. Optimisation of DOX loading onto SC nanoparticles

There are several methods to prepare chitosan nanoparticles of which anion-cation polyelectrolyte complex (PEC) formation is the most often used [17]. Earlier, we showed that PEC is always formed when ChiNPs interact with any substances with the opposite charge such as proteins or peptides [13]. As DOX has a zeta-potential around +7 mV, we selected negatively charged SCNPs (-25 mV) as a carrier for DOX. We tried to load DOX during SCNP formation or onto preformed particles by varying the DOX concentration from 50 to 500 µg/ml and SC concentration from 200 to 500 µg/ml. Loading of DOX during SCNP formation resulted in less than 5% of sorption in all combinations, while the particles themselves were successfully formed. Loading of DOX on preformed SCNPs produced better results (***Figure 2***). Maximal sorption was found to be 50-60% when 30-40 µg/ml of DOX and 200 µg/ml of SCNPs was used during the loading. The dilution of SCNP-DOX in 0.9% NaCl and 1 h incubation at 22 °C and 37 °C led to partial desorption of 30% and 60% of DOX, accordingly.

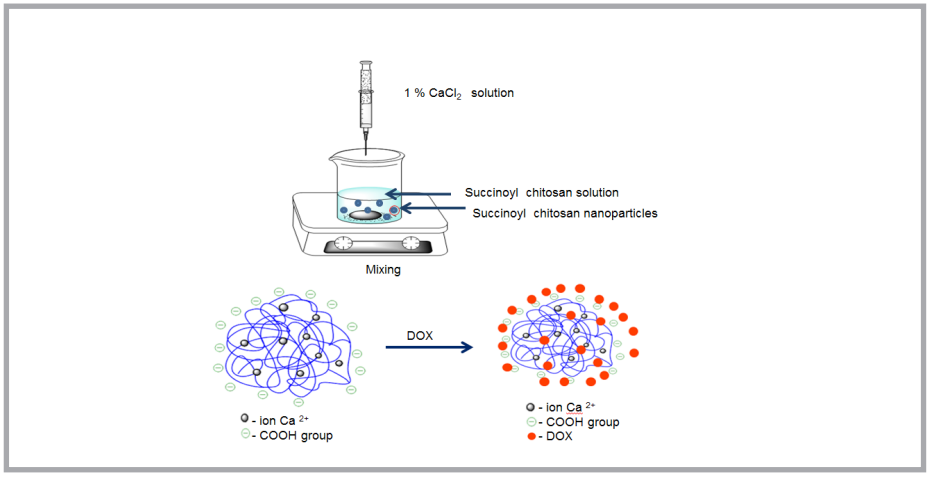

Figure 2. *Schematic illustration of DOX loading onto preformed succinoyl chitosan nanoparticles.*

3.2. Characterisation of SCNPs and SCNP-DOX

SCNPs and SCNP-DOX were analysed by dynamic light scattering (DLS), nanoparticle tracking analysis (NTA), and phase-modulation laser interference microscopy (PLIM). As demonstrated earlier, ChiNPs, as well as molecular Chi, demonstrate bi-modal profiles with peaks of 150 - 200 nm and 600 - 800 nm when analysed by DLS, as found by many other authors [13, 18]. In our experiments, we also found two populations by DLS analysis with 186 and 700 nm in diameter (***Figure 3.a***). However, SCNPs were distributed as a single population with a peak at 119 nm with slightly wider polydispersity when analysed by NTA (***Figure 3.c***) [19]. The process of particle formation is linear and depends on Chi derivatives and counteragent concentrations. Newly formed particles can aggregate, but the aggregates may contain various numbers of nanoparticles, otherwise there must be some mechanisms regulating DLS bi-modal distribution. NTA demonstrated that aggregates were distributed randomly with rare particles larger than 500 nm in diameter (***Figure 3.c***). We concluded that SCNPs form a single polydisperse population, as shown by NTA analysis.

DOX loading did not change the particle size and distribution significantly. We demonstrated that the loading of DOX slightly increased the average size of SCNPs from 119 to 134 nm (***Figure 3.d***). These results were correlated by DLS method when the average size on SCNP increased from 186 to 219 nm (***Figure 3.b***).

It was of interest to visualise SCNP-DOX using a new technique of phase-modulation laser interference microscopy [20]. PLIM permits not only visualisation of nanoparticles but also analysis of their internal structure by the gradient filtration of phase images.

PLIM analysis demonstrated that SCNP-DOS had a round to oval form (***Figure 3.e***) with a dense PEC zone around the hollow centre of the particle (***Figure 3.f***).

3.5. Biodistribution study

In our previous experiments, we studied the dynamics of particle accumulation in different organs of mice after i.v. injection and demonstrated that a steady-state condition was achieved within 1 h. In this experiment, mice were sacrificed 1 h after SCNP-DOX injection to limit the decay of DOX *in vivo*. Control mice were used to estimate the auto-fluorescence of different organs which depended significantly on the organ: kidney > liver > lung > tumour > brain > spleen. Auto-fluorescence was subtracted from all corresponding samples from mice injected with SCNP-DOX. A calibration curve using free DOX dissolved in the extraction buffer was used to estimate the amount of DOX extracted from a corresponding organ. Livers and tumours were homogenised in 4 ml of saline, while other organs were homogenised using 1 ml. Final calculation included a dilution factor of 4 to compensate the result for liver and tumour samples. Thus, the amount of DOX was estimated per full organ and then divided per organ weight to obtain the total concentration of DOX per gram of tissue. We collected only the major organs which are usually considered to accumulate nanoparticles.

When comparing the biodistribution of free DOX and SCNP-DOX via the i.v. route, we found out that SCNP-DOX delivered significantly more DOX into tumours and less into kidneys and the liver (Figure 4 A). Accumulation of DOX in spleen and lungs was

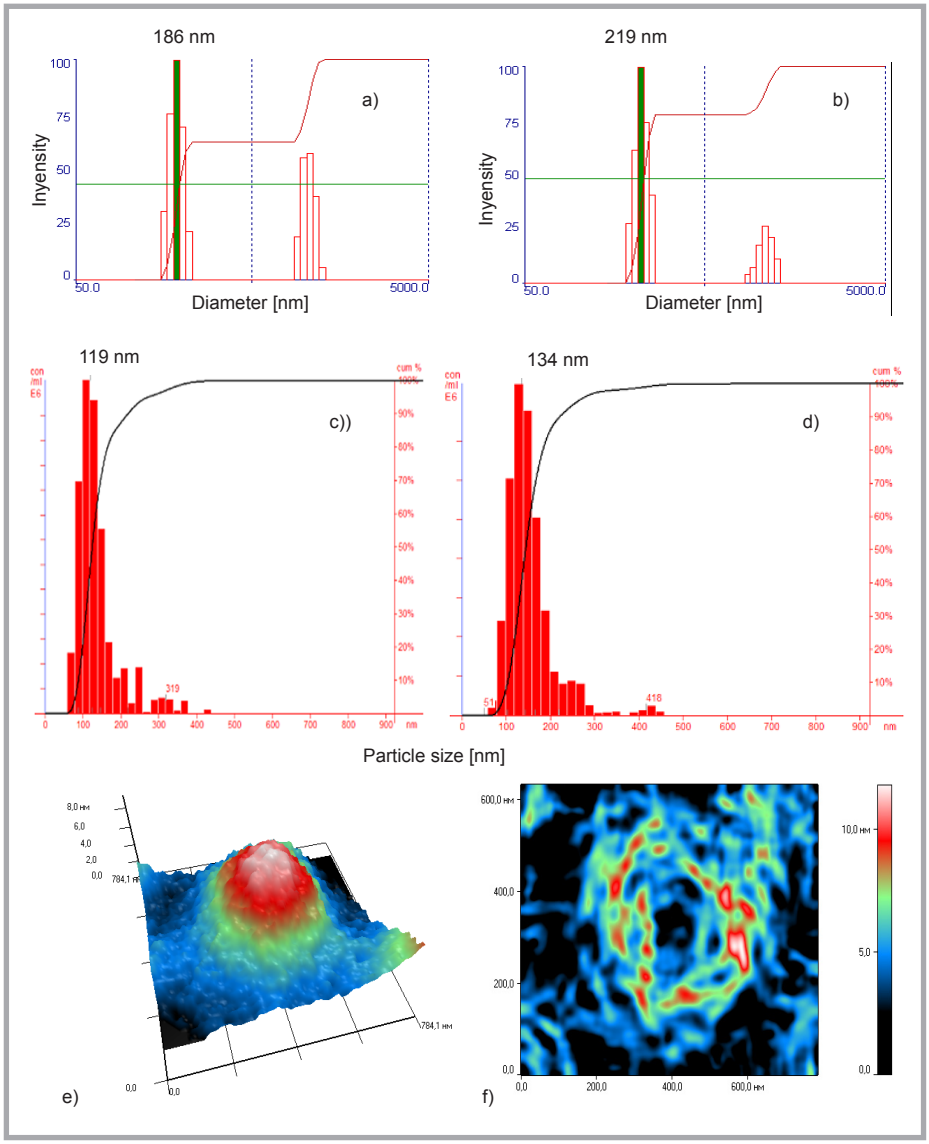

Figure 3. *Dynamic light scattering (A, B), nanoparticles tracking analysis (NTA) (C, D) and phase-modulation laser interference microscopy (PLIM) (E, F) of SCNPs (A, C) and SCNP-DOX (B, D-F).*

comparable, while no DOX was found in brains both after free DOX or SCNP-DOX injections. Contrary to the i.v. route, the biodistribution of SCNP-DOX instilled i.n. was completely different (***Figure 4.b***). We found significantly less SCNP-DOX in the spleen and more in the lungs and brains of experimental mice in comparison with the free DOX

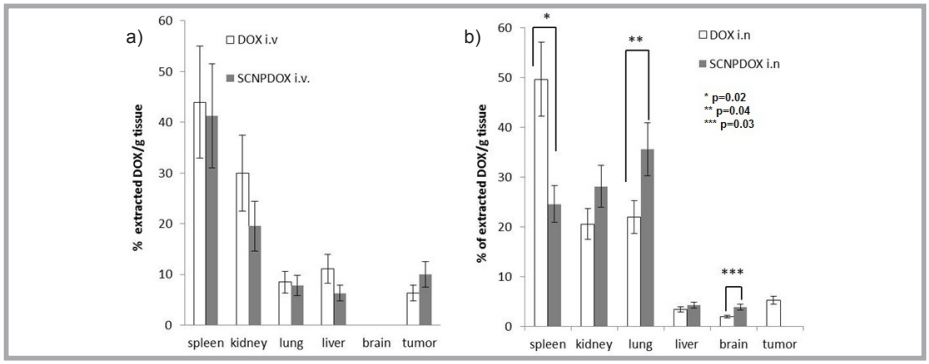

Figure 4. *In vivo biodistribution DOX and SCNPs – DOX administrated intravenous (a) and intranasal (b).*

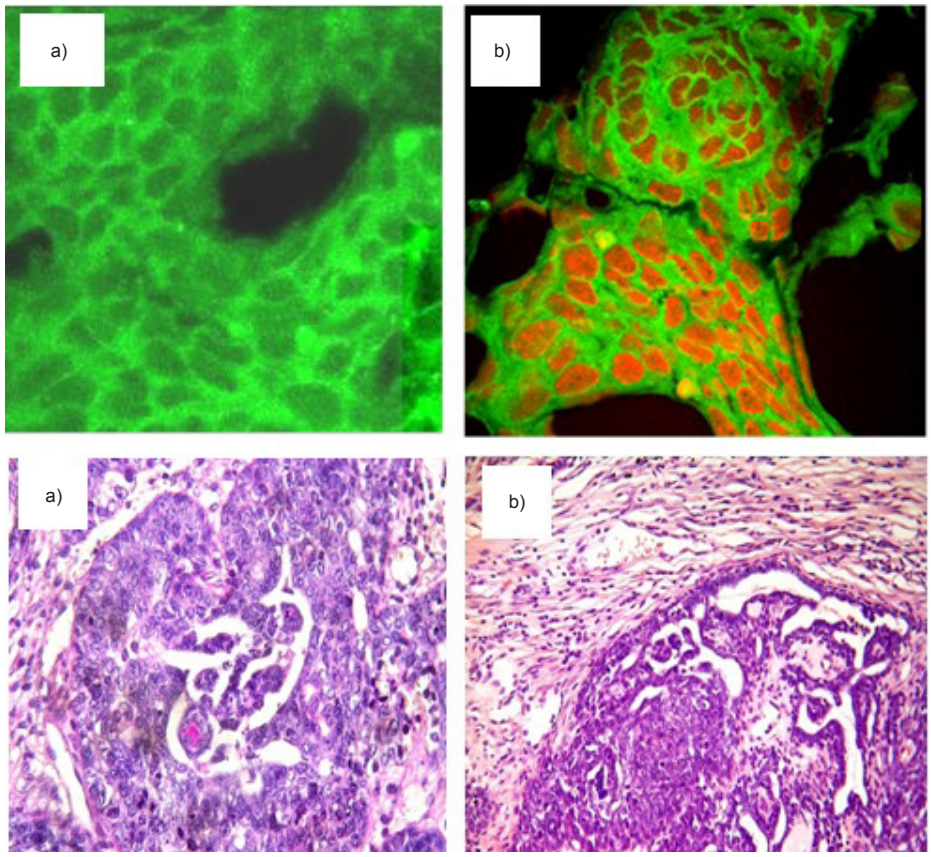

Figure 5. *Cryosections (a, b) and histology (c, d) of tumour tissue after i.n. (a, c) and i.v. (b, d) administration of SCNPs –DOX. Cytoplasm of cells in cryosections was stained with 10-N-nonyl acridine orange (3000×). Histology is stained with H&E (100×).*

group. It is of note that free DOX penetrated BBB when introduced by the i.n. route. The second finding was the absence of SCNP-DOX in the peripheral tumour after i.n. instillation (***Figure 5***). Taken collectively, we supported the results of previously published papers that significantly more DOX penetrates BBB after i.n. delivery by NPs. However, our results on biodistribution in organs after i.n. route of introduction differ from the results obtained by Md et al. [12]. Evidently, more studies are required to get a better understanding of the biodistribution of ChiNPs.

4. Conclusions

We have developed 120 - 200 nm in diameter succinoyl chitosan based delivery system for doxorubicin as well as for other positively charged molecules. Incorporation of DOX slightly increased the size of the particles. We supported the previously published data on the different biodistribution of particles after i.v. and i.n. delivery with significantly increased amounts of NPs in brains in the i.n. groups. However, we did not identify the distribution of NPs into tumours after i.n. instillation. Thus, selection of a delivery route can modify the outcome of therapy.

5. Acknowledgments

This work was supported by President Grants for Government Support of Young Russian Scientist, 2012-2014. We are grateful to Pavel Ignatyev (AMPHORA Laboratories, Russia) for the MIM study and N.A. Nikitin and E.A. Trifonova (Biology Department, Lomonosov Moscow State University, Moscow) for the characterization of particles by NTA.

6. References

1. Agnihotri S.A., Mallikarjuna N.N., Aminabhavi T.M.; (2004). Recent advances on chitosan-based micro- and nanoparticles in drug delivery. J Control Release, 100, 5–28, DOI: 10.1016/j.jconrel.2004.08.010.
2. Amidi M., Romeijn S.G., Borchard G., Junginger H.E., Hennink W.E., Jiskoot W.; (2006). Preparation and characterisation of protein-loaded N-trimethyl chitosan nanoparticles as nasal delivery system. J Control Release, 111, 107–116, DOI: 10.1016/j.jconrel.2005.11.014.
3. Balabushevich N.G., Pechenkin M., Shibanova E.D., Volodkin D.V., Mikhalchik E.V.; (2013). Multifunctional polyelectrolyte microparticles for oral insulin delivery. Macromol Biosci., 13, 1379-1388, DOI: 10.1002/mabi.201300207.
4. Sáenz L., Neira-Carrillo A., Paredes R., Cortés M., Bucarey S., Arias J.L.; (2009). Chitosan formulations improve the immunogenicity of a GnRH-I peptide-based vaccine. Int J Pharm., 369, 64–71, DOI: 10.1016/j.ijpharm.2008.10.033.
5. Liang N., Sun S., Li X., Piao H., Piao H., Cui F., Fang L.;(2012).α-Tocopherol succinate-modified chitosan as a micellar delivery system for paclitaxel: preparation, characterisation and in vitro/in vivo evaluations. Int J Pharm., 423, 480–488, DOI: 10.1016/j.ijpharm.2011.12.004.
6. Cho Y., Kim J.T., Park H.J.; (2012). Size-controlled self-aggregated N-acyl chitosan nanoparticles as a vitamin C carrier. Carbohydr Polym., 88, 1087–1092, DOI: 10.1016/j.carbpol.2012.01.074.
7. Ju Y., Jang J., Woo Y., Chung H., Park R., Chan I., Yong J.; (2003). Biodistribution and anti-tumour efficacy of doxorubicin loaded glycol-chitosan nanoaggregates by EPR effect. J Control Release, 91, 135–145, DOI: 10.1016/S0168-3659(03)00231-1.
8. He C., Hu Y., Yin L., Tang C., Yin C.; (2010). Biomaterials effects of particle size and surface charge on cellular uptake and biodistribution of polymeric nanoparticles. Biomaterials, 31, 3657–3666, DOI: 10.1016/j.biomaterials.2010.01.065.

9. Alhareth K., Vauthier C., Gueutin C., Ponchel G., Moussa F.; (2012). HPLC quantification of doxorubicin in plasma and tissues of rats treated with doxorubicin loaded poly(alkylcyanoacrylate) nanoparticles. J Chromatogr B, 887-888, 128–132, DOI: 10.1016/j.jchromb.2012.01.025.
10. Zhang C., Qu G., Sun Y., Wu X., Yao Z., Guo Q., Zhou H.; (2008). Pharmacokinetics, biodistribution, efficacy and safety of N-octyl-O-sulphate chitosan micelles loaded with paclitaxel. Biomaterials, 29, 1233–1241, DOI: 10.1016/j.biomaterials.2007.11.029.
11. Pardeshi C.V., Belgamwar V. S.; (2013). Direct nose to brain drug delivery via integrated nerve pathways bypassing the blood-brain barrier: an excellent platform for brain targeting. Expert Opin Drug Deliv., 10, 957–972, DOI: 10.1517/17425247.2013.790887.
12. Md S., Khan R.A., Mustafa G., Chuttani K., Baboota S., Sahni J.K., Ali J.; (2012). Bromocriptine-loaded chitosan nanoparticles intended for direct nose to brain delivery: Pharmacodynamic, Pharmacokinetic and Scintigraphy study in mice model. Eur J Pharm Sci., 48, 393–405, DOI: 10.1016/j.ejps.2012.12.007.
13. Zubareva A., Ily'ina A., Prokhorov A., Kurek D., Efremov M., Varlamov V., Svirshchevskaya E.; (2013). Characterization of protein and peptide binding to nanogels formed by differently charged chitosan derivatives. Molecules, 18, 7848–64, DOI:10.3390/molecules18077848.
14. A. V. Il'ina, A. A. Zubareva, D. V. Kurek, A. N. Levov, and V. P. Varlamov ; (2012). Nanoparticles based on succinyl chitosan with doxorubicin: preparation and properties. Nanotechnology in Russia, 7, 85-92, DOI: 10.1134/S1995078012010107.
15. Svirshchevskaya E.V., Mariotti J., Wright M.H., Viskova N.Y., Telford W., Fowler D.H., Varticovski L.; (2008). Rapamycin delays growth of Wnt-1 tumours in spite of suppression of host immunity. BMC cancer, 8, 176, DOI:10.1186/1471-2407-8-177.
16. Long L.W., Times C., Gabizon A., Shioia R., Papahadjopoulos D.; (1989). Pharmacokinetics and tissue distribution of doxorubicin encapsulated in stable liposomes with long circulation times. J Natl Cancer Inst., 81, 1484–1488, DOI:10.1093/jnci/81.19.1484.
17. Bhattarai N., Gunn J., Zhang M.; (2010). Chitosan-based hydrogels for controlled, localised drug delivery. Adv Drug Deliv Rev., 62, 83–99, DOI: 10.1016/j.addr.2009.07.019.
18. Zhang L., Zhao Z.-L., Wei X.-H., Liu J.-H.; (2013). Preparation and in vitro and in vivo characterization of cyclosporin A-loaded, PEGylated chitosan-modified, lipid-based nanoparticles. Int. J Nanomedicine., 8, 601–10, DOI: 10.2147/IJN.S39685.
19. Zubareva A.A., Kurek D.V., Sizova S.V., Svirshchevskaya E.V., Varlamov V.P.; (2012). Characterization of physicochemical parameters. Nanotechnology in Russia, 7, 428–433.
20. Brazhe A.R., Brazhe N., Maksimov G.V, Ignatyev P.S., Rubin A.B., Mosekilde E., Sosnovtseva O.V.; (2008). Phase-modulation laser interference microscopy: an advance in cell imaging and dynamics study. J Biomed Opt., 13, 034004, DOI:10.1117/1.2937213.